Vol. **2**, **2**. 157-162 (2010)

Revue de Mécanique Appliquée et Théorique

Elastoplastic behaviour of zirconium alloy cladding tubes after cold rolling

J. Fajoui
GeM, Institut de Recherche en Génie Civil et Mécanique, Université de Nantes, Ecole Centrale de Nantes, CNRS UMR 6183, 37 Boulevard de l'Université, BP 406, 44 602 Saint-Nazaire, France

D. Gloaguen
GeM, Institut de Recherche en Génie Civil et Mécanique, Université de Nantes, Ecole Centrale de Nantes, CNRS UMR 6183, 37 Boulevard de l'Université, BP 406, 44 602 Saint-Nazaire, France,
david.gloaguen@univ-nantes.fr

E. Girard
GeM, Institut de Recherche en Génie Civil et Mécanique, Université de Nantes, Ecole Centrale de Nantes, CNRS UMR 6183, 37 Boulevard de l'Université, BP 406, 44 602 Saint-Nazaire, France

R. Guillén
GeM, Institut de Recherche en Génie Civil et Mécanique, Université de Nantes, Ecole Centrale de Nantes, CNRS UMR 6183, 37 Boulevard de l'Université, BP 406, 44 602 Saint-Nazaire, France

Abstract
Complementary methods have been used to analyse residual stresses in zirconium alloy tubes which were manufactured by cold rolling: X-ray diffraction and scale transition model. A modified elasto-plastic self-consistent model (EPSC) has been used to simulate the experiments and exhibits agreement with experimental data. X-ray diffraction analysis in rolling direction shows different stress values for the analysed planes respectively. The measured strains were generated by an anisotropic plastic deformation. Plastic incompatibility stress on X-ray measurements should be taken into account so as to make a correct interpretation of the experimental data.

Résumé
Le comportement élastoplastique de tubes en alliage de zirconium, mis en forme par laminage à pas de pèlerin, a été étudié en utilisant la diffraction des rayons X couplée à un modèle de transition d'échelles. Une approche élastoplastique autocohérente avec une nouvelle formulation de la plasticité cristalline a été mise en place pour simuler le comportement du matériau. L'influence et le rôle de l'anisotropie plastique ont pu être analysés et expliqués. Les simulations ont permis de reproduire l'évolution de la texture et délimiter les contributions des contraintes du premier et du second ordre sur les valeurs déduites de la diffraction.

1. INTRODUCTION

Pressurized heavy water reactors use zirconium alloys due to their low neutron absorption cross-section, low irradiation creep and high corrosion resistance in reactor atmosphere. Due to their hcp structure, Zr single crystals are usually highly anisotropic. Consequently, strong residual stresses are generated in fabricated components of Zr alloy during mechanical treatments. These stresses play an important role in subsequent deformation and modify the mechanical properties of the reactor core components. This work concerns the manufacturing process of Zr alloy cladding tubes. These tubes

are manufactured by cold rolling. To reach its final size, the material undergoes three cold-rolling passes in a particular mode called cold pilgering. To understand the influence of plastic anisotropy on the mechanical properties, the last rolling pass has been completely studied. X-ray diffraction techniques are used to characterize the mechanical state at the macro- and meso-scopic levels of the specimens. The experimental data show the appearance of important second order stresses which depend on crystallographic planes. A modified EPSC approach is adopted to describe the plasticity evolution and determine the active deformation systems. A formulation of the crystal behaviour is proposed. Experimental results have been compared with those given by the modified model for Zr alloy tubes. The EPSC formulation provides an accurate description of the intergranular plastic residual stresses induced by the anisotropic plastic behaviour of single crystals. An estimation of the first-order stresses is also proposed.

2. MODIFIED SELF-CONSISTENT APPROACH

The plastic flow can take place when the Schmid criterion is verified, i.e. slip occurs if the resolved shear stress τ^g on a system *g* is equal to the critical value τ_c^g depending on the hardening state of the slip system. A complementary condition which states that the increment of the resolved shear stress must be equal to the incremental rate of the critical resolved shear stress (CRSS) has to be verified simultaneously. In small strain formulation, one has:

$$\dot{\tau}^g = R^g..\sigma \ = \tau_c^g \qquad \text{and} \qquad \dot{\tau}^g = R^g..\dot{\sigma} \ = \dot{\tau}_c^g \tag{1}$$

where R^g is the Schmid tensor on a system g and ".." is the double scalar product. If $\dot{\gamma}^g$ denotes the slip rate on a system g, the Schmid criterion is thus given by:

$$\tau^g < \tau_c^g \Rightarrow \dot{\gamma}^g = 0 \tag{2.a}$$

$$\tau^g = \tau_c^g \text{ and } \dot{\tau}^g < \dot{\tau}_c^g \Rightarrow \dot{\gamma}^g = 0 \tag{2.b}$$

$$\tau^g = \tau_c^g \text{ and } \dot{\tau}^g = \dot{\tau}_c^g \Rightarrow \dot{\gamma}^g > 0 \tag{2.c}$$

The main problem is to determine which combination of slip systems will be really activated at each step of the plastic deformation path. In this case, all possible combinations of potentially active systems have to be scanned to find one that satisfies the two preceding conditions simultaneously. Running time considerations become the main task of the model. From the work of Ben Zineb et al. [1], the relations (2a), (2b) and (2c) can be expressed with the following equation:

$$\dot{\gamma}^g = M^g \dot{\tau}^g \tag{3}$$

The slip rate is linked to the resolved shear stress through a function M^g. This formulation is based on the crystalline rate-dependent flow rule. On the other hand, the time variable does not play any role in this approach. The hardening parameter M^g is given by:

$$M^g = \beta\left[\frac{1}{2}\left(1+\text{th}\left(k_0\left(\frac{\tau^g}{\tau_c^g}-1\right)\right)\right)\right]\left[\frac{1}{2}((1+\text{th}(k_0\dot{\tau}^g))\right]\left[\frac{1}{2}(1+\text{th}(k_0\tau^g))\right] \tag{4}$$

From equation (4) and after some algebraic calculations, the constitutive relation which links the overall stress rate and strain rate in the grain is then given by:

$$\dot{\varepsilon} = \left[s + \sum_g (R^g..M^g..R^g)\right]..\dot{\sigma} = \ell^{-1}..\dot{\sigma} \tag{5}$$

Here appears the elastoplastic consistent tangent module tensor ℓ. The other mechanical variables are determined by the usual relations given by the EPSC model [2], taking into account the equations (3) and (5).

3. EXPERIMENTAL PROCEDURE

3.1 Crystallographic texture analysis

X-ray diffraction analysis has been performed with a four circle XRD3003PTS SEIFERT goniometer. The K_α copper radiation has been used as the X-ray. The study of samples having a curved geometry not only requires an accurate positioning of the samples but also takes into account the geometric effects induced by XRD directional feature. A theoretical model based on a ray-tracing method was used to take into account the geometric effects which modify the collected intensities [3]. Correction coefficients accounting for the "geometrical texture" of the samples as well as absorption corrections are calculated for each measurement point. Figure 1 presents the initial and final textures. In the final state, the {0002} PF shows a bimodal distribution of the intensity maxima in the NT-TD plane at about 30° of the ND axis. This is typical for this kind of sample.

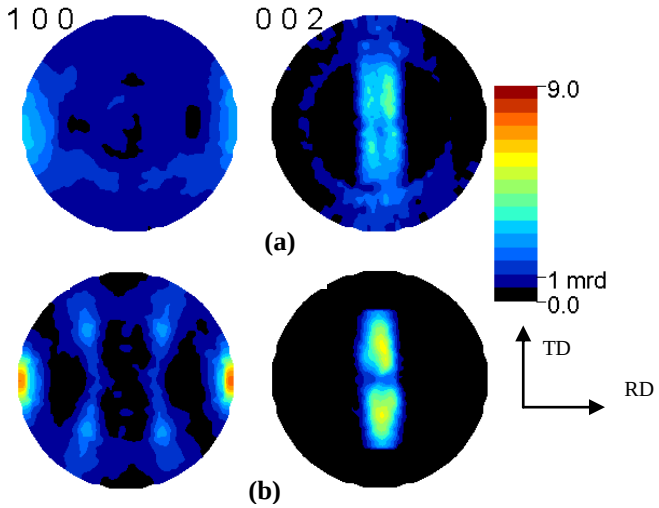

Figure 1: Initial (a) and final (b) { 0002 } and { $10\bar{1}0$ } PF.

3.2 Evaluation of residual stresses

The average strain for diffracting grains can be written as [4]:

$$\left\langle \varepsilon(\phi,\psi,\mathrm{hkil})\right\rangle_{V_d} = F_{ij}(\phi,\psi,\mathrm{hkil})\sigma^{I}_{ij} + \left\langle \varepsilon^{IIpi}(\phi,\psi,\mathrm{hkil})\right\rangle_{V_d} \quad (6)$$

$< >_{Vd}$ is the average over diffracting grains for the hkil reflection. $F_{ij}(\phi,\psi,hkil)$ are the X-ray elastic constants and $\left\langle \varepsilon^{IIpi}(\phi,\psi,\mathrm{hkil})\right\rangle_{V_d}$ the mean value of strain incompatibilities between the diffracting and the non diffraction volumes. σ^I is the macroscopic stress tensor.

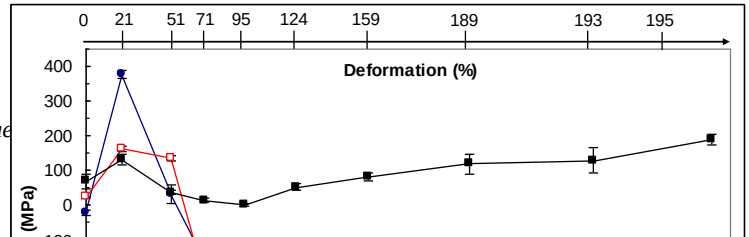

(a)

(b)

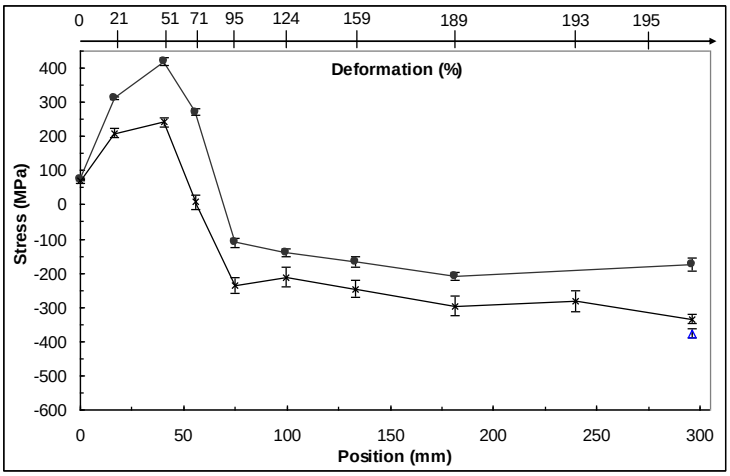

Figure 2: experimental longitudinal stress $\sigma_{11}^{exp}(hkil)$ calculated with the relation (6) ($\left\langle \varepsilon^{IIpi}(\phi,\psi,hkil)\right\rangle_{V_d}$ = 0) and obtained with different crystallographic planes. (a): ■-{ $10\bar{1}4$ }, □-{ $20\bar{2}2$ }, •-{ 0004 } (with Cr radiation). (b): •-{ $20\bar{2}5$ }, Δ-{ $30\bar{3}2$ }, ×-{ $21\bar{3}3$ } (with Cu radiation).

The second term in the above equation can be approximated by:

$$\left\langle \varepsilon^{IIpi}(\phi,\psi,hkil)\right\rangle_{V_d} = q\left\langle \varepsilon^{IIth}(\phi,\psi,hkil)\right\rangle_{V_d} \quad (7)$$

where $\left\langle \varepsilon^{IIth}(\phi,\psi,hkil)\right\rangle_{V_d}$ is calculated from the EPSC model and averaged for crystallites having the (hkil) normal to the orientation characterized by the ψ and ϕ angles. q is a constant factor (a fitting parameter) introduced in order to find the real magnitude of plastic strains. In this case, it is possible to evaluate the magnitude of the first as well as the second order residual stresses using eqs. (6,7) with a non-linear fitting procedure associated with the scale transition model. Relation (6) shows clearly that the measured strain cannot be identified with the macroscopic strain if the material presents anisotropic properties. The presence of intergranular strain after a mechanical solicitation influences the measured strain. Generally, the interpretation of experimental data is based on the unjustified assumption that $\left\langle \varepsilon^{IIpi}(\phi,\psi,hkil)\right\rangle_{V_d}$ = 0. We have determined the evolution of internal stresses due to

plastic anisotropy in deformed samples along the rolling direction for the last rolling step at different total strain levels. These experiments were carried out on a XRD3003PTS SEIFERT goniometer with Cr K_α and Cu K_α radiations. An Ω goniometric assembly with a position Sensitive Detector was used. Three plane families were studied with Cr radiation: $\{10\bar{1}4\}$ at 2θ = 156.7°, $\{20\bar{2}2\}$ at 2θ = 137.2° and $\{0004\}$ at 2θ = 125.6°. With Cu radiation, the three plane analysed were: $\{20\bar{2}5\}$ at 2θ = 136.8°, $\{30\bar{3}2\}$ at 2θ = 123.0° and $\{21\bar{3}3\}$ at 2θ = 117.8°. The direction ϕ = 0° corresponds to the rolling direction (parallel to the tube axis). Figure 2 shows the evolution of residual stress for each plane as a function of the axial position z along the rolling direction (z varies between 0 and 300 mm).

4. SIMULATION DATA

The texture was introduced in the model by a set of 1000 grains characterized by Euler angles and by weights which represent their volume fraction. The main active slip systems are assumed to be: the prismatic systems, the first-order pyramidal slip (pyr<c+a> and pyr<a>) and $\{10\bar{1}2\}$ twinning. The critical resolved shear stresses (CRSS) used here, τ = 95 MPa for prismatic mode, τ = 175 MPa for pyr<a>mode, τ = 310 MPa for pyr<c+a> slip system and τ = 180 MPa for tensile twinning, give a correct description of the experimental data. We considered a linear hardening law [5,6], the coefficient H^{gr} being equal to H^{gg} for any deformation mode r: $\dot{\tau}^g = H^g \sum_r \dot{\gamma}^r$. The hardening coefficients were found to be 80 MPa for prismatic slip, 170 MPa and 300 MPa for pyramidal slip (pyr<a>and pyr<c+a> respectively) and 180 MPa for twin mode.

5. RESULTS

Applying eq. (6) and (7) and fitting the results from the model to the experimental data, the longitudinal stress σ_{11}^I and the q factor have been found for each step of the rolling process. Table 1 gives the result for the final tube (195% total deformation). σ_{11}^I value reaches 60 MPa. In order to express the influence of the second order plastic strain on the correct interpretation of experimental data an additional test has been performed. The procedure presented above has been applied for the X-ray measurements but with the assumption [that] $\left\langle \varepsilon^{IIpi}(\phi,\psi,hkil)\right\rangle_{V_d}$ = 0. The results are presented in table 1. For σ_{11}, the two planes exhibit an opposite behaviour: traction for $\{10\bar{1}4\}$ plane and compression for $\{20\bar{2}2\}$ plane. X-ray measurements show the effective existence of plastic anisotropy. As can be seen from eq. (6), the measured stress depends on a function of the analysed plane family.

Strain incompatibilities are present at the mesoscopic level in the material and consequently, the stresses obtained by XRD depend on the plane. The diffracting crystals are not the same for each case, which allows us to deduce that different second order stresses exist, linked to a strong anisotropic plastic deformation for these two plane families. The term $\left\langle \varepsilon^{IIpi}(\phi,\psi,hkil)\right\rangle_{V_d}$ plays a key role in a correct interpretation of different measurements of residual stresses. The method employed in this study enables the magnitude of the macro- and meso-scopique residual stresses to be evaluated using information from an EPSC approach.

	q	σ^{I}_{11} (MPa)	
$\left\langle \varepsilon^{IIpi}(\phi,\psi,hkil)\right\rangle_{V_d} \neq 0$	0.202 ± 0.081	60 ± 30	
$\left\langle \varepsilon^{IIpi}(\phi,\psi,hkil)\right\rangle_{V_d} = 0$	-	$\{10\bar{1}4\}$ plane	$\{20\bar{2}2\}$ plane
		189 ± 16	-226 ± 24

Table 1: results of evaluation of σ^{I} and q parameter with two different assumptions, i.e. $\left\langle \varepsilon^{IIpi}(\phi,\psi,hkil)\right\rangle_{V_d} = 0$ or $\neq 0$.

6. CONCLUSIONS

A modified algorithm has been used for computing the mechanical response of a single crystal. Numerical results, obtained at the different scales, show the relevance of this approach. This approach has been developed in order to simulate the mechanical response of Zr alloy tube after cold pilgering. Stresses observed by X-ray diffraction are significantly different from one plane family to another. These results can be explained by the presence of mesoscopic stresses of plastic in the material. A self-consistent model had been used to quantify the stress differences between these plane families. The choice of prismatic slip as principal deformation mode can explain the opposite pseudo-macrostresses values for the two studied planes. These predicted results can only be obtained for a single set of slip modes and hardening parameters. This analysis shows that X-ray diffraction stress analysis could constitute an effective validation or identification of a model. Nevertheless, the influence of second order strain must be taken into account to get a correct interpretation of X-ray diffraction results for hexagonal material.

7. REFERENCES

1 Ben Zineb T., Arbab Chirani S., Berveiller M.: Nouvelle formulation de la plasticité cristalline utilisant une contrainte de référence avec écrouissage, fifteenth French conference of mechanic, Nancy, France, 2001.

2 Schmitt S., Lipinski P.: Modelling of the elasto-plastic behavior of rolled aluminium alloy for forming applications, J. Mat. Tech., 74, 14-22, 1998.

3 Guillén R., Cossu C., Jacquot T., François M., Bourniquel B.: X-ray diffraction texture analysis of cylindrical samples, J. Appl. Cryst., 32, 387-392, 1999.

4 Baczmanski A., Hfaiedh N. François M., Wierzbanowski K.: Plastic incompatibility stresses and stored elastic energy in plastically deformed copper,, Mater. Sci. Eng. A, 501, 153-165, 2009.

5 Pang J. W. L., Holden T.M., Turner P.A., Masson T.E.: Intergranular stresses in Zircaloy-2 with rod texture, Acta Mater., 47, 373-383, 1999.

6 Gloaguen D., François M., Guillén R.: Mesoscopic residual stresses of plastic origin in zirconium: interpretation of X-ray diffractions results, J. Appl. Cryst., 37, 934-940, 2004.